

# Computational Model of Hole Transport in DNA

Maksym Volobuyev<sup>†</sup> and Ludwik Adamowicz<sup>\*,‡,§</sup>

Nano-Biomolecular Engineering Science and Technology (n-BEST) Program and Department of Chemistry, University of Arizona, Tucson, Arizona 85721, and Dipartimento di Chimica e Chimica Industriale, Università di Pisa, via Risorgimento, 35, I-56126 Pisa, Italy

Received: June 29, 2004; In Final Form: October 20, 2004

A computational model based on the molecular dynamics (MD) simulation for the hole transport in DNA has been developed and applied to study hole current in DNA strands consisting of different numbers of GC pairs. The approach is based on the hopping mechanism which is thermally activated. The calculations show that the hole hopping intensifies with the temperature and the transport rate increases in agreement with the experimental evidence. It is also determined that the degree of structural ordering in the DNA strand enhances the hole conductivity and reasons are provided why this may occur.

## 1. Introduction

The process of charge transport through DNA strands has been intensively studied for over a decade. The experiments of Giese et al.<sup>1–4</sup> and Yoo et al.<sup>5</sup> have shown that electrons and holes may migrate along the DNA chain for long distances. This means that, if a charge is injected at some place in the DNA strand, it may easily migrate to other even very distant locations. There are important consequences of this phenomenon to the DNA physical and chemical behavior including processes involved in the DNA oxidative and radiative damage and its repair. In the latter process the long-distance electron transfer from an electron donor to the damage site is a key element in the repair mechanism. The DNA repair processes play a vital role in the survival of living cells and our understanding of these processes at the molecular may have far-reaching consequences to the development of agents and procedures for dealing with medical problems centered in the DNA. The importance of these processes has inspired a large body of biological and medical research directed to studies of mutagenic changes and their chemistry.<sup>6</sup> Another reason the DNA charge transport has been recently investigated is related to the DNA application outside biology. The self-assembly, replication properties, and structural integrity of DNA have been recognized as desirable featured for nanotechnology applications. For example, natural and synthetic structures where DNA plays a role of an active element have been investigated for their use as “molecular wires” in nano-electronic applications.<sup>7,8</sup>

It has been postulated that two different mechanisms operate in the process of charge transfer through inhomogeneous, structurally flexible molecular systems such as DNA.<sup>9</sup> The first mechanism is the charge tunneling effect which can be explained by the quantum nature of the electrons and their behavior in the molecular systems. This mechanism plays an important role only in charge transfer over short distances in DNA when the charge source and the charge destination are separated by only a few nucleobase pairs. The second mechanism is the thermally activated hopping process which dominates in charge-transfer events in DNA occurring over long distances.<sup>1</sup> It has been shown

that the molecular dynamics (MD) simulation can be a useful tool to investigate this mechanism.<sup>10,11</sup> In our own investigations concerning the electron transport in DNA, we have used this technique, and the results we obtained have been fully consistent with the available experimental data concerning the temperature dependency of the electron transport rates the DNA systems.<sup>12</sup>

Since the hole transport (i.e., the transport of the positive charge) may play an even more important role in the DNA electrical conductivity than the transport of excess electrons, in this work, we have extended the MD approach previously used to study the DNA electron conductivity to model DNA hole transport. Although the electron and the hole transport processes are similar, because they both involve transferring electrons between molecular units forming the DNA strand, there are some important differences. The main difference is related to the fact that the former process involves excess electron propagation through unoccupied DNA orbitals (LUMOs), whereas the transfer of the holes involves propagation of electrons through DNA HOMOs.

As the model systems for the investigation, we have chosen strands consisting of only GC basis pairs, i.e., the (GC)<sub>n</sub> strands. This choice was dictated by the known property of the guanine nucleobase to possess the lowest ionization potential of all the DNA bases. Thus, if a hole appears in the DNA strand, it would preferentially localize and move through guanines instead of other bases in the process of the charge transport.

In the approach we employed, the classical MD simulation was used to describe the hole transfer in DNA through the hopping mechanism. The hole migration in this mechanism involves an electron transfer from a neutral guanine molecule to a neighboring guanine cation. Thus, as a prerequisite to MD simulations, a series of quantum mechanical (QM) calculations were performed to determine the energy of the electron removal from the neutral guanine molecule and the energy associated with electron attachment to the guanine cation at different geometrical configurations of those systems. The QM calculation will be described in the next section.

## 2. QM Calculations

As mentioned, in this work, we focus on describing the DNA hole-transport dynamics over long distances. As it was shown<sup>10,11</sup>

\* To whom correspondence should be addressed.

<sup>†</sup> University of Arizona.

<sup>‡</sup> Università di Pisa.

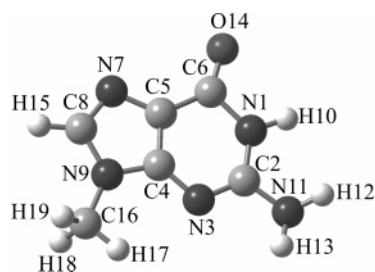


**Figure 1.** Equilibrium structure of the N9-methylguanine molecule.

this type of dynamics can be very well represented in the first approximation by the thermally induced hopping model implemented in the MD simulation method. Besides the charge transport, the MD method has been widely and successfully applied to investigate other dynamical DNA properties.<sup>13</sup>

In simulating the dynamics of the DNA charge conductivity, it is important to have a good description of the interaction of the DNA units with excess electrons and holes. This particularly applies to the DNA domains that are directly involved in the charge localization and transport. In the electron transfer process, those directly involved parts are thymine or cytosine moieties and in the hole transport those are the guanine units. Hence, as a prerequisite to the MD simulation of the hole conductivity, the hole–guanine interaction has to be described in QM calculations at the level that ensures an adequate representation of the interaction not only at the equilibrium but also in situations when the guanine moiety is distorted from the equilibrium geometry by thermal fluctuations.

In the calculations of the hole–guanine interaction (i.e., in the calculations of the neutral guanine molecule and its cation), we have used a system that better resembles the guanine moiety that occurs in the DNA helix than the isolated guanine molecule. This better model is the N9-methylguanine molecule that has the hydrogen in the 9th position substituted by a methyl group to simulate the guanine connection to the sugar moiety in the DNA strand. The molecular structure of N9-methylguanine is shown in Figure 1.

The Gaussian 98<sup>14</sup> package was used for the QM calculations performed in this work. The vibrational analysis and the calculation of the normal modes were also done with Gaussian 98. The interaction of an electron with the rest of the molecule is an effect that is sensitive to the electron correlation. However, a large number of single-point calculations that we needed in this work precluded application of a high-level *ab initio* method (such as the coupled cluster method). Thus, the density functional theory (DFT) method with the B3LYP functional was used in the calculations. That level of theory was used before in similar calculations by others.<sup>12,15</sup>

Previous studies have shown that the 6-31+G\* basis set is a reasonable choice for calculating structures and first-order properties of DNA components.<sup>12</sup> It is known that a good representation of the HOMOs is important to correctly describe processes involved in the hole transfer. Wetmore et al.<sup>15</sup> showed that inclusion of a full set of polarization functions for the valence shells of all atoms in the system in the DFT calculation increases the IPs for the nucleobase by, on average, 0.19 eV. Thus in this work, we used the standard 6-31G\*\* basis set that should provide an adequate level of accuracy in describing the hole–guanine interaction in DFT/B3LYP calculations.

The first DFT/B3LYP calculations performed in this work concerned the geometry optimizations of the neutral N9-methylguanine molecule and its cation. At that level of theory, both systems have planar ring framework. This is different from

**TABLE 1: N9-Methylguanine Energies in Vacuo at Different Equilibrium Geometries. IP for the Neutral Guanine Molecule and VEA for Its Cation<sup>a</sup>**

	at neutral equilibrium geometry		at cation equilibrium geometry
neutral	−581.879453	neutral	−581.868719
cation	−581.602296	cation	−581.615639
VIP	7.54	VEA	6.89

<sup>a</sup> Total energies in a.u.; IP and VEA in eV.

the situation in some covalent anions of the nucleic acid bases which are known to display some degree of ring puckering upon covalent attachment of an electron. It does not seem likely that electron removal leads to a similar ring-deformation effect in the nucleic acid bases.

As mentioned, guanine is the nucleobase with the lowest ionization potential (IP) of all of the nucleic acid bases. The experimental value of the guanine IP (8.20 eV<sup>16</sup>) was reproduced with acceptable accuracy by several calculations.<sup>15,17,18</sup> Our vertical IP (VIP) of 7.54 eV (see Table 1) agrees well with the values obtained by others (for example, with the value of 7.51 eV reported in ref 17). We should mention that some underestimation of the absolute value of the guanine IP in our calculations is not that important because in our hole conductivity model, the relative difference between the guanine IP and the vertical electron affinity (VEA) of the guanine cation, and not the absolute values of these quantities, is used as the parameter controlling the hole transport process. Since, as can be expected, the VIPs and VEAs are subject to similar underestimation in our calculations, the error in their difference is likely to be much smaller than the error in their absolute values. The vertical electron affinity (VEA) of the guanine cation is shown in Table 1. This quantity has not been reported by others, but we needed it in our approach since its comparison with the VIP (calculated for the neighboring base) determines whether a hole hopping is to occur in the DNA strand. It should be noted that  $|VIP| - |VEA| = 0.65$  eV (with the VIP and VEA determined at the equilibrium geometries of the respective systems) is a rather large difference for a thermal activation hopping. However, when a guanine molecule is placed in the DNA strand its geometry changes due to the interactions with the surrounding molecular environment and the energy gap between IP and VEA decreases.

The main problem we are facing in the MD simulation of the hole hopping in the (CG)<sub>n</sub> chains is the need to calculate the VEA of the guanine base where the hole is located and the VIPs of the two neighboring guanine bases in each time-step of the MD simulation to determine if the hole hopping will occur. These calculations have to be repeated at each time step because the structures of the guanines change due to thermal fluctuations. The VEA and VIP calculations cannot be done by using the DFT procedure because this would take too much time. Thus, we had to apply a procedure that, like in our previous work on the electron transport,<sup>12</sup> was based on using polynomial expansions of the guanine-neutral and guanine-cation total DFT/B3LYP energies in terms of the normal modes of these systems. The procedure is described below.

The equilibrium geometries of the neutral N9-methylguanine molecule and its cation are reference points in our MD calculations (we also called them the reference geometries). Any configuration of the guanine molecule,  $g(t)$ , in the DNA strand that may occur during the MD simulation as a result of thermal motions at a particular time step  $t$  can be approximated by a displacement of the guanine equilibrium geometry,  $g_{eq}$ , along the normal vibrational modes according to the following equation:

$$g(t) = g_{\text{eq}} + \sum_{i=1}^M \alpha_i(t) g_{\text{disp}}^i \quad (1)$$

Here  $g_{\text{eq}}$  denotes the standard equilibrium geometry of N9-methylguanine represented in terms of Cartesian coordinates,  $M$  (equal to 51 for N9-methylguanine) is the number of normal vibrational modes,  $\alpha_i(t)$  are weight factors, and  $g_{\text{disp}}^i$  are standard displacements along normal modes which are obtained from the vibrational analysis performed using Gaussian 98.

As it was shown in our previous work,<sup>12</sup> transition energies (e.g., the vertical electron affinity) are not always symmetrical functions in terms of the direction of the displacement of the molecule along a normal vibrational mode (i.e., not symmetric in terms of positive and negative  $\alpha_i(t)$  values). The asymmetric character of the transition energies was enhanced by nonplanarity of the thymine anion structure at equilibrium in our previous calculations concerning the electron transport.<sup>12</sup> In Figure 1 in the Supporting Information, we show, for example, the energy of N9-methylguanine as function of the distortion along the  $\text{NH}_2$ -group symmetric vibration. For approximating this curve, as well as the energy curves corresponding to displacing the molecule along other normal modes, we used a sixth-order polynomial expansion

$$E_i(\alpha_i) = E_0 + \sum_{j=1}^6 c_{ij}(\alpha_i)^j; \quad i = 1, \dots, M \quad (2)$$

Our analysis has shown that 6th degree polynomial provides an adequate extrapolation function in the range of the distortions along the normal modes that are relevant for the present calculations. The polynomial coefficients have been determined using a standard mean-square minimization procedure using twenty energy points calculated along each vibrational mode.

Polynomial approximations have been determined for the following energy functions: (a) the energy of the neutral N9-methylguanine as functions of the displacements of its structure along the normal mode from its equilibrium geometry; (b) the energy of the neutral N9-methylguanine as functions of the displacements of its structure along the normal modes determined for the N9-methylguanine cation from the equilibrium geometry of the cation; (c) the energy of the N9-methylguanine cation as functions of the displacements of its structure along the normal coordinates determined for the neutral N9-methylguanine from the equilibrium geometry of the neutral; and (d) the energy of the N9-methylguanine cation as functions of the displacements of its structure along the normal modes determined for the cation from the equilibrium geometry of the cation.

To describe the hole hopping in the MD calculations a procedure had to be developed and implemented in the MD simulation program that calculates the VEA of the guanine cation where the hole is located in the DNA strand and the VIPs of its two neighboring neutral guanine molecules. The VEA and VIP values had to be calculated at the geometries of the cation and the neutral systems that the MD procedure produced at each step of the simulation. These VEA and VIP values were calculated according to the following algorithm that used the above-described four groups of energy functions for the neutral N9-methylguanine and its cation parametrized in terms of the normal modes and approximated by the 6th degree polynomials.

1. At every step of the simulation, the MD procedure produces a new DNA geometry in terms of the atomic Cartesian coordinates of all of the molecular units in the DNA strand including the guanine moieties and the guanine cation moiety

where the hole is located. For the guanine cation and for the two neighboring guanine neutral molecules, those geometries were extracted from the MD procedure and stored (we will refer to them as “current structures”). Next in each of the three geometries the bond that in the DNA exists between N9 and the sugar residue was replaced by a methyl group. The geometry of the methyl was taken to be its equilibrium geometry. This step produced three N9-methylguanine structures, two neutral and one cation with their corresponding geometries given in terms of the Cartesian coordinates.

2. In the next step, the Cartesian geometries of the three structures were transformed to the “standard orientation” form by appropriate translations and rotations. In this transformation, the center of mass of each system was first moved to coincide with the origin of the coordinate system and rotated to satisfy the Eckart<sup>19</sup> conditions with respect to the reference N9-methylguanine equilibrium structure either corresponding to the neutral molecule or the cation (represented here by the set of  $3N$ -coordinate vector  $g_{\text{eq},i}$ ,  $i = 1, 19$ ; the reference structures were described in the beginning of this section)

$$\sum_{i=1}^{19m_i} g_i = 0 \quad (3)$$

$$\sum_{i=1}^{19m_i} [g_{\text{eq},i}(g_i - g_{\text{eq},i})] = 0 \quad (4)$$

In the above equations  $m_i$  are the masses of the atoms and  $g_i$  and  $g_{\text{eq},i}$  are the Cartesian geometries of the current N9-methylguanine structure extracted from the MD simulation and the reference structure, respectively. After applying the Eckart transformation, any translation and/or rotation of the current structure with respect to the reference structure was excluded from the consideration. Thus after the transformation, the Cartesian geometry of the guanine extracted from the DNA strand in the current step of the MD simulation differed from the reference N9-methylguanine geometry only in terms of vibrational displacements.

3. For the given geometry of the N9-methylguanine molecule, the set of the weight parameters,  $\alpha_i$ , defined by eq 2 were now calculated by projecting the geometry-difference vector,

$$\Delta g = \sqrt{m}(g - g_{\text{eq}}) \quad (5)$$

onto the normal coordinates,  $Q_i$

$$\alpha_i = Q_i \Delta g \quad (6)$$

4. In each step of the MD simulation, the above procedure was applied to the guanine cation where the hole was located and to the two neighboring neutral guanines. For each of the three systems, two sets of  $\alpha_i$  parameters were determined, one to describe the geometry of the system in terms of the normal-mode displacements from the equilibrium (reference) geometry of the neutral N9-methylguanine and the other one in terms of the normal-mode displacements from the equilibrium (reference) geometry of the N9-methylguanine cation. Having the two sets of the parameters, the total energies of the cation and the neutral system at the current geometry of the system were estimated from the polynomial approximations. From those two energies, the VIP for neutral system and the VEA for the cation was obtained.

The above algorithm was coded in FORTRAN and implemented in the AMBER<sup>20</sup> program package. The calculations



described in the next section were carried out using this augmented AMBER program.

### 3. Molecular Dynamics Simulations

**3.1. System Description.** The MD calculations were carried out for  $\beta$ -DNA (GC) $_n$  duplexes with different lengths. As it was shown by Giese et al.<sup>1</sup> and by Bixon and Jortner,<sup>9</sup> for a short DNA strand ( $n < 4$ ) the tunneling is the main mechanism the charge moves along DNA. Since the hopping starts to dominate in longer chains, in the present investigations we have considered DNA strands with four, seven, and ten CG base pairs ( $n = 4, 7$ , and  $10$ ). Due to the hopping mechanism is temperature-activated, the temperature effect on the hole transport rate was one of the main focuses of the investigation. The calculations were carried out at the same three different temperatures used before in our previous study of the DNA electron transport.<sup>12</sup> In the case of the electron transport, our MD calculations showed that 300 K was the lowest limit for the electron transfer to occur due to the thermally activated hopping. Below 300 K the thermal internal vibrations of the thymine in the (AT) $_n$  DNA strand were not distorting the molecule strong enough to allow the VEA and VDE curves to cross and facilitate an electron hopping between two thymine residues. The question we ask in the present work, is whether a similar effect operates in the thermally activated hole transport in (GC) $_n$  DNA strands and, if it does, at what temperature it occurs. In the test calculations, we raised the temperature even to 400 K, which is a very high for the DNA aqueous solutions, to study the effect such extreme conditions may have on the DNA charge transport.

As mentioned, all present calculations were carried out with the AMBER 6.0 package augmented with the additional procedure describing the hole transport through the hopping mechanism. The AMBER package has been a useful tool in studies of the dynamics of biological systems in many investigations. The Cornell et al.<sup>21</sup> force field was used for the DNA strand and the TIP3 force field for water. In those models the total energy  $E_{\text{tot}}$  is a sum over bonded ( $E_b$ ) and nonbonded ( $E_{\text{nb}}$ ) interactions

$$E_b = \sum_{\text{bonds}} K_r(r - r_{\text{eq}})^2 + \sum_{\text{angles}} K_\theta(\theta - \theta_{\text{eq}})^2 + \sum_{\text{dihedrals}} 0.5V_p[1 + \cos(p\phi - \lambda)] \quad (7)$$

$$E_{\text{nb}} = \sum_{j < i} \left[ \frac{A_{ij}}{R_{ij}^{12}} - \frac{B_{ij}}{R_{ij}^6} + \frac{q_i q_j}{R_{ij}} \right] \quad (8)$$

For correcting the long-range electrostatic interactions, we used the Ewald summation procedure.

At the beginning of the MD calculation, the DNA strand was built in AMBER by a standard procedure implemented in that program. Next, the atomic charges on guanine atoms (see Table 1 in the Supporting Information) were altered to make them consistent with the representation of the guanine molecule in the module of the program that simulated the hole hopping. In the standard implementation AMBER, the HF/6-31+G\* atomic charges are used, whereas the VIP and VEA calculations for describing the hole hopping in this work were done using the DFT/B3LYP/6-31G\*\* level of theory. Hence we replaced the charges in the RESP procedure by the charges obtained with DFT/B3LYP/6-31G\*\*. Additional slight adjustment was also required in the charge distribution of the methyl group in N9-methylguanine because the total charges on the methyl and on

sugar-phosphate backbone were not equal. To alleviate this problem and balance the charge, the excess charge from the backbone was equally distributed over all atoms of the guanine molecule. The above modifications of the charges made our charges on the DNA atoms slightly different from same atomic charges in the standard AMBER model.

In constructing the model of the DNA strand for the MD calculation, a guanine cation was always placed in the first base pair in the strand. Next, counterions were added in appropriate places and water molecules were included using the standard solvation procedure implemented in AMBER. In that procedure, water molecules are included into a parallelepiped box with the DNA strand in the center of the box. The distance between any atom on the DNA surface and the closest box boundary was not less than 8.0 Å.

**3.2. The Method.** Each MD calculation was initiated with the energy minimization (thermal cooling) of the system. The duration of the cooling was about 50 ps and during that time the system was coupled to a 300 K Berendsen thermostat with the relaxation time equal to 2 ps. This was the starting point for further thermalization. From this point, the system was allowed to evolve along the phase trajectory over the period of 100 ps to the equilibrium point. Such a long time for this initial step was required because a high degree of structure relaxation was needed for the charge transfer modeling to be performed. The time step in the modeling was chosen to be 0.001 ps. That should be sufficiently small to achieve adequate accuracy of the simulation.

When the equilibrium point was achieved in the MD simulation, the hole transfer process was initiated in the calculation. As mentioned, a positive charge was placed on the first guanine molecule in the strand and the hole transfer procedure was turned on. In this procedure, in each MD simulation step including the first one, the VEA for the guanine cation, where the hole was localized, was determined using the energies of the guanine neutral and guanine cation parametrized in terms of the normal modes of the systems. In the same way, the VIPs of the neighboring guanine molecules (in the first and the last step there was only one such molecule; in other steps there were two such molecules) were determined. We allowed the hole transfer to occur in the simulation only if the following transition condition was satisfied:

$$\Delta E = |\text{VEA}| - |\text{VIP}| > t_d \quad (9)$$

where  $t_d$  is a threshold. If the condition (9) was satisfied for both guanines, the hole was moved to the one with higher VIP.

We should mention here that our DNA conductivity study concerns situations where the charge transport in the DNA strand is induced by a potential bias applied to the two ends of the strand. This bias was represented here in the same way as it was done in our previous work on the DNA electron conductivity,<sup>12</sup> i.e., by using a lower threshold value for the forward movement of the hole along the strand than for the backward movement. In the present calculations, the threshold for the backward hole transition was set to 0.003 au and for the forward transition it was set to 0.001 au. The use of the thresholds for the hole transfer not only allowed us to effectively represent the presence of the electric field but also allowed for effective representation of the tunneling barrier that the hole may encounter in hopping between two adjacent guanines. One should notice that, even if an electric field is applied along the DNA strand, our procedure still allows the hole to move backward in the strand against the field if the condition (9) permits it. This is consistent with the experimental evidence

**TABLE 2: Average ( $\tau_{\text{hop}}^{\text{aver}}$ ) and Instantaneous ( $\tau_{\text{hop},f}^{\text{inst}}$ ,  $\tau_{\text{hop},b}^{\text{inst}}$ ) Hopping Times for (GC) $_n$  Systems at Different Temperatures**

<i>n</i>	$\tau_{\text{hop}}^{\text{aver}}$			$\tau_{\text{hop},f}^{\text{inst}}$			$\tau_{\text{hop},b}^{\text{inst}}$		
	300 K	350 K	400 K	300 K	350 K	400 K	300 K	350 K	400 K
4	4.67	2.86	2.82	5.02	4.23	3.38			
7	4.58	4.41	3.54	4.28	3.88	4.35	3.72	4.00	
10	4.49	5.16	4.48	5.04	4.43	4.06	3.48	3.97	

obtained by Furrer and Giese<sup>4</sup> showing that after injection in the middle part of strand the hole can move in both directions. In our model, we did not use any charge delocalization procedure as it was done by Renger<sup>22</sup> only because our previous calculations<sup>23,24</sup> have shown that the charge is strongly localized at one of the bases with the other basis playing the role of a solvating agent that stabilizes the excess charge.

After the hole transfer is initiated in the MD calculation, it continues to move through hopping between neighboring guanine molecules until it eventually reaches the other end of the (GC) $_n$  strand (i.e., the 3' end). When the condition (9) is satisfied and the hole hopping takes place, the guanine with the hole is neutralized and one of the two adjacent guanines is ionized. This process changes the interaction potential in the MD simulation. In particular, it changes the force field for the guanine cation, that now becomes a neutral system, as well as for the neutral guanine that loses an electron to become a cation. Essentially, to accommodate these changes, the force field for the cation has to be switched to the force field of the neutral molecule and that of the adjacent neutral guanine that becomes ionized has to be switched to the force field of the cation. Such a switching procedure was been implemented in the MD simulation in AMBER.

In the calculations we performed three MD simulations for each (GC) $_n$  system. The results of the calculations are described and discussed in the next section.

#### 4. Discussion

The calculations showed that the hole transport occurs at every temperature for which the MD simulation was performed. This means that the intensity of the molecular vibrations was high enough to overcome the energy gap between the VIP of the neutral guanine and the VEA of the guanine cation. We define two lifetimes to characterize the hole transfer process in the DNA strand as described by the MD simulations performed in this work. The first lifetime corresponds to how long, on average, the hole stays on a particular guanine before a hopping to the next guanine occurs ( $\tau_{\text{hop}}^{\text{inst}}$ ). To determine this quantity, several MD runs were performed and after excluding some lowest (below 1 ps) and some highest results (over 10 ps) the averaged  $\tau_{\text{hop}}^{\text{inst}}$  was determined. The averaging was done separately for the forward hole transfer ( $\tau_{\text{hop},f}^{\text{inst}}$ ) and the backward transfer ( $\tau_{\text{hop},b}^{\text{inst}}$ ).

The second lifetime we calculated here was the average lifetime for the hole hopping in a particular MD simulation run ( $\tau_{\text{hop}}^{\text{aver}}$ ). It can be calculated as

$$\tau_{\text{hop}}^{\text{aver}} = \frac{\tau_{\text{tot}}}{N} \quad (10)$$

where  $\tau_{\text{tot}}$  is the total time the hole needs to transfer from the 5' to the 3' end of the DNA strand, and  $N$  is the number of hopping events that occurred in the simulation of this event.

As one can see from Table 2, all lifetimes decrease when the

temperature increases. This behavior may be explained by the increased intensity of the molecular vibrations with the temperature and more frequent crossings of the VIP and VEA curves for the two guanines that exchange the hole. Larger changes observed in shorter strands indicate stronger structural correlations between G–C pairs inside those structures than in longer strands. In longer strands, the structure relaxation takes more time because the movement of even closely located guanine molecules inside the strand is almost independent. In the short chains, the state of the terminal G–C pair plays an important role because it is located, on average, closer to the other pairs than in the longer strands. The atomic vibrations of these molecules are strongly coupled with the surrounding water molecules resulting in an effect that propagates through out the whole strand. Naturally, this affects the shorter strands more than the longer strands.

An important consequence of the structure rearrangement due to the hole transport can be demonstrated by comparing  $\tau_{\text{hop},f}^{\text{inst}}$  and  $\tau_{\text{hop},b}^{\text{inst}}$ . For the (GC) $_4$  strand,  $\tau_{\text{hop},b}^{\text{inst}}$  cannot be determined because the charge moves in this strand through a system with a high degree of the internal order. In such a case, one can describe the electrical properties of the strand as consistent with properties of a second-type conductor characterized by a very low conductance. When the chain length becomes longer, the degree of ordering decreases or even vanishes resulting in each hopping step becoming longer than for the shorter strands since more structure change is required to create favorable conditions for a hole hop. High temperature may accelerate that change and the average time between two hops may significantly decrease. But this only works for  $\tau_{\text{hop},f}^{\text{inst}}$  because the hopping process in the backward direction may be sensitive to other factors and is less frequent than the forward hopping. We discuss this point next.

The use of different thresholds for hole transfer in opposite directions brings some anisotropy into the simulation of the hopping process. In this, there is one effect that we should mention. At the point when a hopping step occurs, the VIP of the neutral guanine molecule is almost equal to the VEA of the adjacent guanine cation. Even when the hole jumps to the next position, the system still remains in the configuration it was before the hop. We can say that it, in a way, “remembers” that position. If the temperature is not high enough and the structure relaxation is not happening fast enough, there is a possibility that a backward jump may occur before the conditions become favorable for the next forward jump. It is because the next guanine molecule located in the forward direction needs some time (around 1 ps) to “realize” the presence of the charge at the neighboring position and to adjust its structure to receive the hole. At higher temperatures, this time is smaller because the structural changes happen faster than at lower temperatures. Thus, with temperature increasing the forward jumps become more frequent. At the same time, the probability of the backward jumps is reduced. It lead to decrease of the  $\tau_{\text{hop},f}^{\text{inst}} - \tau_{\text{hop},b}^{\text{inst}}$  difference. For all our systems, the noted tendency has appeared.

It is worthwhile to note that in our model there are two factors that determine whether at a particular MD step the hole proceeds forward or backward in its hopping movement along the strand or whether it stays at the current base pair and does not move. The first factor is the difference between the energy gain associated with the hole moving to the next base pair located in the forward direction in the strand vs the energy gain associated with the hole moving to the next base pair located in the backward direction (the  $\Delta E_f$  and  $\Delta E_b$  quantities, respectively). We can call this factor a thermodynamic factor

**TABLE 3: Averaged Total Time,  $\tau_{\text{tot}}$ , and Number of Hops,  $N_{\text{hop}}$ , Needed for a Hole to Transfer through Whole DNA Strand**

$n$	$\tau_{\text{tot}}$			$N_{\text{hop}}$		
	300 K	350 K	400 K	300 K	350 K	400 K
4	37.14	16.55	14.96	8.3	6.3	5.0
7	110.98	141.38	78.35	23.3	33.0	22.0
10	52.02	113.91	171.19	11.7	23.7	38.3

because it describes the probability of the hole moving in the forward or the backward direction. The second factor is the hopping barrier defined by the forward and backward thresholds ( $t_b$  and  $t_f$ ). This is a kinetic factor which represents activation energy for the hopping process.

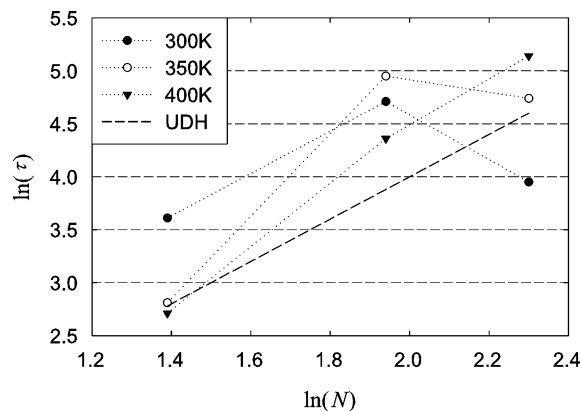
In order for a hole to hop, either  $\Delta E_b > t_b$  or  $\Delta E_f > t_f$  must occur. If both conditions are satisfied, the hole hop is made to occur in the MD simulation in the direction leading to its lower energy after the hop (recall that  $t_b > t_f$ ). If a forward motion of the hole occurs, this can mean that the both thermodynamic and kinetic factors favor the forward motion and disfavor the backward motion. However, the forward hole motion is also possible if the two factors oppose each other, but the kinetic factor is stronger than the thermodynamic factor, i.e., the situation when the hole would lower its energy more by moving backward than forward, but the lowering is only large enough to overcome the forward barrier and not enough to overcome the backward barrier. Thus a backward motion in our MD simulation can only occur if it is strongly favored by the thermodynamic factor because the kinetic factor always works against the backward jump. Our calculations showed that a large fraction of the forward hops occur due to the kinetic preference and against the thermodynamic factor which often favors the backward motion.

The lifetimes discussed above describe the charge transfer between the nearest guanine molecules. But, based on the results of the simulations, we can also derive some conclusions concerning the hole transfer through the whole strand. The total transfer time,  $\tau_{\text{tot}}$ , and the total number of hops,  $N_{\text{hop}}$ , are integral characteristics of the whole charge transport process. As one can see from Table 3,  $\tau_{\text{tot}}$  for the (GC)<sub>4</sub> system decreases when the temperature increases, whereas for the (GC)<sub>10</sub> system, the opposite takes place. As mentioned before, in (GC)<sub>4</sub> there is more structural correlation (structural order) than in (GC)<sub>10</sub>, and the forward hole transport is more preferred. In (GC)<sub>10</sub> there is lower structural order particularly in the middle part of the strand. In this middle part the mechanism of the charge transfer resembles random walking with the frequency of hopping in either direction being more closely related to the system temperature. Comparing  $N_{\text{hop}}$ 's for (GC)<sub>4</sub> and (GC)<sub>10</sub> supports this observation. (GC)<sub>7</sub> seems to be an intermediate case where no clear dependency on either the chain length or temperature can be observed.

The lifetimes describing a dynamical molecular process are closely related to the rate of the process. This relation plays an important role because models of the molecular mechanism for the process can be developed based on the information on the rate.<sup>17,25</sup> In studies of the short distance charge transfer through DNA strands, an exponential distance-dependence of the rate has been observed. The exponential rate is consistent with the tunneling mechanism of the process

$$k \approx k_0 e^{-\beta NR} \quad (11)$$

Here  $k$  is the donor–acceptor charge-transfer rate,  $k_0$  is the rate when the donor and acceptor are in contact,  $R$  is a distance

**Figure 2.** Lifetime–distance dependency at different temperatures.

between two adjacent nucleobases in the strand,  $N$  is the number of the base pairs in the strand, and  $\beta$  is a parameter characteristic for the process. For the long-range charge transfer in DNA, where the thermally activated hopping mechanism starts to dominate, a different relation between the process rate and the number of base pairs needs to be used

$$k \approx \tau^{-1} N^\eta \quad (12)$$

where  $\tau$  is the lifetime and  $\eta$  is a power parameter.

In such a model the lifetime  $\tau_{\text{tot}}$  should be a linear function of  $N$  on the logarithmic scale. As one can see from Figure 2, this is true only for the highest temperature considered in the calculations. Meanwhile, in our previous work on the electron transport in DNA,<sup>12</sup> we obtained almost perfect linear dependencies of the electron transfer rate for all of the temperatures used in the simulations. There is an explanation why the hole transport would behave differently at lower temperatures than the electron transport. The explanation concerns the difference in the charge transfer mechanism. As was shown above, the hole transport through a DNA strand strongly depends on the structure relaxation, whereas this effect plays a smaller role in the electron transfer. The temperature increase affects the structure relaxation time by making it occur faster and this reduces the role of this factor in the hole transfer mechanism at the highest temperature making it more similar to the mechanism operating in the case of the electron transfer.

According to Jortner et al.,<sup>25</sup> there are three main charge-transfer mechanisms which can be distinguished by different values of the parameter  $\eta$  (see eq 12):

1. For the unbiased diffusive hopping (UDH)  $\eta = 2$ ;
2. For the acceptor direction-biased random walk (ADRW)  $1 \leq \eta \leq 2$ ;
3. For the donor direction-biased random walk (DDRW)  $\eta \geq 2$ .

For the electron transfer,  $\eta = 1.68$  was obtained in our previous study,<sup>12</sup> and it was consistent with either the UDH or the ADRW mechanism in Jortner's theory. As mentioned, for the hole hopping studied in the present work, one can see a linear dependency only at the highest temperature 400 K. In this case,  $\eta = 2.70$  and we can conclude that the DDRW model applies here. This is consistent with setting  $\tau_{\text{hop},f}^{\text{inst}} > \tau_{\text{hop},b}^{\text{inst}}$  which preferentially moves holes in the donor direction. At lower temperatures, however, due to less intense thermal motion of the system, the structural relaxation becomes slower and the structural coupling between the DNA units decreases. By this we mean the following. Say, the current position of the hole is the G in the base pair 3. The neighboring base pairs 2 and 4 "feel" the presence of the hole at 3 and their structures are



adjusted in response to the interaction with the hole (this is what we mean by the coupling). Now, let us consider a situation when the hole moves to the 4th base pair. In the MD simulation it takes some time for the base pairs 3 and 5 to adjust to the presence of the positive charge at 4. It also takes some time for the base pair 2 to decouple from the state it was when the hole was located at 3. All these coupling and decoupling processes may take several MD steps, but the process is faster at higher temperatures. We can say that, on average, the structural readjustment is achieved (through coupling between the base pair with the hole and the two neighboring base pairs) more quickly at higher temperatures than at lower temperatures. These effects apparently result in a considerable change of the charge-transfer mechanism with the temperature, which is showing in the way the rate depends on the length of the strand at different temperatures.

## 5. Conclusion

In this work we described an MD procedure for simulating electric-field-induced migration of positive charge through DNA strand by the hopping mechanism. Within this model, we described and explained the temperature and chain-length dependencies of some parameters representing the strand electrical conduction. The parameters are the average lifetimes a hole stays at a single guanine residue in DNA and the average lifetime it takes for the hole to transfer through the whole length of the chain. The analysis of the DNA structural changes in the hole conduction process indicates that the presence of a long-range order in the DNA strand in the 300–350 K temperature range is an important factor that may affect the conductivity. This order decreases or completely disappears in longer DNA strands.

The structural order in DNA can be investigated by means of the correlation functions (atomic radial distribution and velocity autocorrelation functions) routinely obtained in MD simulations. Another way to investigate this feature is by comparing the results obtained for dry and wet DNAs. Since the presence of water molecules in the DNA strand enhances the autocorrelation tendency, including different levels of hydration in the model may provide a good way to study the correlation effects in the MD calculations. If long-range correlation plays an important role in the DNA conductivity, as this study suggests, the presence of factors enhancing the correlation and the structural order in DNA may be a way to increase the DNA conductivity and make it into a true molecular wire.

There is a number of ways the present model can be improved. Including a better solvent description would certainly make the model more realistic. One can also improve the interaction potential (9) by including polarizabilities in the formula. Another way the approach can be improved is by explicitly including water molecules in the DFT calculations of the VIP and VEA of guanine. This may help explaining the well-known “trapping” effects<sup>1</sup> which occur when a hole jumps from the DNA strand to a cluster of water molecules and the hole transfer is terminated. Making the model more complex is going to result in a larger calculation cost. However, new more efficient techniques are being worked out by several groups to address the problem of solvation in QM/MD calculations<sup>26</sup> and

we are planning to incorporate those techniques in our future works on the DNA conductivity.

**Acknowledgment.** This work has been supported by funding provided to the n-BEST program by the University of Arizona and by the NSF NIRT grant.

**Supporting Information Available:** Energy of N9-methylguanine as function of the distortion along the NH<sub>2</sub>-group symmetric vibration (Figure 1). Atomic charges (in a.u) of guanine used in the standard AMBER parametrization and the charges used in our model (Table 1). This material is available free of charge via the Internet at <http://pubs.acs.org>.

## References and Notes

- (1) Giese, B.; Spichty, M.; Wessely, S. *Pure Appl. Chem.* **2001**, *73*, 449.
- (2) Giese, B.; Biland A. *Chem. Commun.* **2002**, 667.
- (3) Giese, B. *Chem. Biol.* **2002**, *6*, 612.
- (4) Furrer, E.; Giese, B. *Helv. Chim. Acta* **2003**, *86*, 3623.
- (5) Yoo, K.-H.; Ha, D. H.; Lee J.-O.; Park, J. W.; Kim, Jinhee; Kim, J. J.; Lee, H.-Y.; Kawai, T.; Choi, Han Yong *Phys. Rev. Lett.* **2001**, *87*, 198102.
- (6) Loft, S.; Poulsen, H. E. *J. Mol. Med.* **1996**, *74*, 297.
- (7) Porath, D.; Bezryadin, A.; de Vries, S.; Dekker, C. *Nature* **2000**, *403*, 635.
- (8) Bashir, R. *Superlattices Microstruct.* **2001**, *29*, 1.
- (9) Bixon, M.; Jortner J. *Chem. Phys.* **2002**, *281*, 393.
- (10) Cizek, J.; Martinez, A.; Ladik, J. *J. Mol. Struct.* **2003**, *626*, 77.
- (11) Pecchia, A.; Gheorghe, M.; Di Carlo A.; Lugli, P.; Niehaus, T. A.; Frauenheim, Th.; Scholz, R. *Phys. Rev. B.* **2003**, *68*, 235321.
- (12) Smith, D. M. A.; Adamowicz, L. *J. Phys. Chem. B.* **2001**, *105*, 9345.
- (13) Mazur, A. K. *J. Comput. Chem.* **2001**, *22*, 457.
- (14) Frisch, M. J.; Trucks, G. W.; Schlegel, H. B.; Scuseria, G. E.; Robb, M. A.; Cheeseman, J. R.; Zakrzewski, V. G.; Montgomery, J. A., Jr.; Stratmann, R. E.; Burant, J. C.; Dapprich, S.; Millam, J. M.; Daniels, A. D.; Kudin, K. N.; Strain, M. C.; Farkas, O.; Tomasi, J.; Barone, V.; Cossi, M.; Cammi, R.; Mennucci, B.; Pomelli, C.; Adamo, C.; Clifford, S.; Ochterski, J.; Petersson, G. A.; Ayala, P. Y.; Cui, Q.; Morokuma, K.; Malick, D. K.; Rabuck, A. D.; Raghavachari, K.; Foresman, J. B.; Cioslowski, J.; Ortiz, J. V.; Stefanov, B. B.; Liu, G.; Liashenko, A.; Piskorz, P.; Komaromi, I.; Gomperts, R.; Martin, R. L.; Fox, D. J.; Keith, T.; Al-Laham, M. A.; Peng, C. Y.; Nanayakkara, A.; Gonzalez, C.; Challacombe, M.; Gill, P. M. W.; Johnson, B. G.; Chen, W.; Wong, M. W.; Andres, J. L.; Head-Gordon, M.; Replogle, E. S.; Pople, J. A. *Gaussian 98*; Gaussian, Inc.: Pittsburgh, PA, 1998.
- (15) Wetmore, S. D.; Boyd, R. J.; Eriksson, L. A. *Chem. Phys. Lett.* **2000**, *322*, 129.
- (16) LeBreton, P. R.; Yang, Xu; Urano, S.; Fetzer, S.; Yu, M.; Leonard, N. J.; Kumar, S. *J. Am. Chem. Soc.* **1990**, *112*, 2138.
- (17) Lewis, F. D.; Letsinger, R. L.; Wasilewski, M. R. *Acc. Chem. Res.* **2001**, *34*, 159.
- (18) Voityuk, A. A.; Jortner, J.; Bixon, M.; Rösch, N. *Chem. Phys. Lett.* **2000**, *324*, 430.
- (19) McCarthy, W. J. Ph.D. Thesis, 1997.
- (20) Case, D. A.; Pearlman, D. A.; Caldwell, J. W.; Cheatham, T. E., III; Ross, W. S.; Simmerling, C. L.; Darden, T. A.; Merz, K. M.; Stanton, R. V.; Cheng, A. L.; Vincent, J. J.; Crowley, M.; Tsui, V.; Radmer, R. J.; Duan, Y.; Pitera, J.; Massova, I.; Seibel, G. L.; Singh, U. C.; Weiner, P. K.; and Kollman, P. A. *AMBER 6*, University of California, San Francisco, 1999.
- (21) Cornell, W. D.; Cieplak, P.; Bayly, C. I.; Gould, I. R.; Merz, K. M.; Ferguson, D. M.; Spellmeyer, D. C.; Fox, T.; Caldwell, J. W.; Kollman, P. A. *J. Am. Chem. Soc.* **1995**, *117*, 5179.
- (22) Renger, T.; Marcus, R. *J. Phys. Chem. A* **2003**, *107*, 8404.
- (23) Jalbout, A. F.; Smets, J.; Adamowicz, L. *J. Chem. Phys.* **2001**, *273*, 51.
- (24) Smets, J.; Jalbout, A. F.; Adamowicz, L. *J. Chem. Phys. Lett.* **2001**, *342*, 342.
- (25) Jortner, J.; Bixon, M.; Langenbacher, T.; Michel-Beyerle, M. E. *Proc. Natl. Acad. Sci.* **1997**, *95*, 12759.
- (26) Scalmani, G.; Barone, V.; Kudin, K.; Pomelli, C. S.; Scuseria, G. E.; Frisch, M. J. *Theor. Chem. Acc.* **2004**, *111*, 90.